NASA/TM—2007-215003

Heat Transfer Analysis of a Closed Brayton Cycle Space Radiator

Albert J. Juhasz
Glenn Research Center, Cleveland, Ohio

August 2007

NASA STI Program . . . in Profile

Since its founding, NASA has been dedicated to the advancement of aeronautics and space science. The NASA Scientific and Technical Information (STI) program plays a key part in helping NASA maintain this important role.

The NASA STI Program operates under the auspices of the Agency Chief Information Officer. It collects, organizes, provides for archiving, and disseminates NASA's STI. The NASA STI program provides access to the NASA Aeronautics and Space Database and its public interface, the NASA Technical Reports Server, thus providing one of the largest collections of aeronautical and space science STI in the world. Results are published in both non-NASA channels and by NASA in the NASA STI Report Series, which includes the following report types:

- TECHNICAL PUBLICATION. Reports of completed research or a major significant phase of research that present the results of NASA programs and include extensive data or theoretical analysis. Includes compilations of significant scientific and technical data and information deemed to be of continuing reference value. NASA counterpart of peer-reviewed formal professional papers but has less stringent limitations on manuscript length and extent of graphic presentations.

- TECHNICAL MEMORANDUM. Scientific and technical findings that are preliminary or of specialized interest, e.g., quick release reports, working papers, and bibliographies that contain minimal annotation. Does not contain extensive analysis.

- CONTRACTOR REPORT. Scientific and technical findings by NASA-sponsored contractors and grantees.

- CONFERENCE PUBLICATION. Collected papers from scientific and technical conferences, symposia, seminars, or other meetings sponsored or cosponsored by NASA.

- SPECIAL PUBLICATION. Scientific, technical, or historical information from NASA programs, projects, and missions, often concerned with subjects having substantial public interest.

- TECHNICAL TRANSLATION. English-language translations of foreign scientific and technical material pertinent to NASA's mission.

Specialized services also include creating custom thesauri, building customized databases, organizing and publishing research results.

For more information about the NASA STI program, see the following:

- Access the NASA STI program home page at *http://www.sti.nasa.gov*

- E-mail your question via the Internet to *help@sti.nasa.gov*

- Fax your question to the NASA STI Help Desk at 301–621–0134

- Telephone the NASA STI Help Desk at 301–621–0390

- Write to:
  NASA Center for AeroSpace Information (CASI)
  7115 Standard Drive
  Hanover, MD 21076–1320

NASA/TM—2007-215003

Heat Transfer Analysis of a Closed Brayton Cycle Space Radiator

Albert J. Juhasz
Glenn Research Center, Cleveland, Ohio

Prepared for the
Fifth International Energy Conversion Engineering Conference and Exhibit (IECEC)
sponsored by the American Institute of Aeronautics and Astronautics
St. Louis, Missouri, June 25–27, 2007

National Aeronautics and
Space Administration

Glenn Research Center
Cleveland, Ohio 44135

August 2007

Acknowledgments

This work was conducted at the NASA Glenn Research Center's Thermal Energy Conversion Branch and at Cleveland State University.

This report is a formal draft or working paper, intended to solicit comments and ideas from a technical peer group.

Level of Review: This material has been technically reviewed by technical management.

Available from

NASA Center for Aerospace Information
7115 Standard Drive
Hanover, MD 21076–1320

National Technical Information Service
5285 Port Royal Road
Springfield, VA 22161

Available electronically at http://gltrs.grc.nasa.gov

Heat Transfer Analysis of a Closed Brayton Cycle Space Radiator

Albert J. Juhasz
National Aeronautics and Space Administration
Glenn Research Center
Cleveland, Ohio 44135

Abstract

This paper presents a mathematical analysis of the heat transfer processes taking place in a radiator for a closed cycle gas turbine (CCGT), also referred to as a Closed Brayton Cycle (CBC) space power system. The resulting equations and relationships have been incorporated into a radiator sub-routine of a numerical triple objective CCGT optimization program to determine operating conditions yielding maximum cycle efficiency, minimum radiator area and minimum overall systems mass. Study results should be of interest to numerical modeling of closed cycle Brayton space power systems and to the design of fluid cooled radiators in general.

Introduction

Due to their relatively low mean effective heat rejection temperature resulting from their characteristic "near isobaric" heat rejection process, Closed Brayton Cycle (CBC) space power systems tend to require large radiator surface areas for a specified heat rejection quantity, as dictated by the cycle temperature ratio and working fluid mass flow rate and the specified by power level. Consequently the radiator and associated heat rejection subsystem accounts for a major fraction of the overall CBC power system mass. Hence a mathematical analysis of the multi-variable heat transfer processes which affect radiator area requirements should provide an important analytical tool in minimizing radiator area and thus arrive at an optimized CBC configuration for given cycle operating conditions.

It is for the above mentioned reasons that a detailed one dimensional analysis of the interacting conduction- convection-radiation heat transfer processes was undertaken. The analysis focuses on the CBC working fluid heat rejection components, consisting of a fluid transport duct penetrated by evaporator sections of heat pipes (HP) which absorb heat from a heat transport fluid flowing over them by convection heat transfer. The finned condenser parts of these HP are located outside the fluid transport duct and are thus exposed to the space environment. It is these HP condenser sections that transfer the cycle reject heat by conduction to high thermal conductivity fins which accomplish the final step in the heat rejection process by thermal radiation to the space environment whose equilibrium sink temperature can be determined (Juhasz 2001).

A literature search of CBC space power systems revealed only sporadic reference to CBC radiator area computation under certain simplifying assumptions. Klann (1970) for example shows an equation for computing radiator area under the assumption of infinite internal heat transfer. This assumption sets internal wall surface temperatures equal to the higher gas temperatures. Hence the radiator average outer wall temperatures are also computed to be higher than their true values resulting in radiator areas that are too low. Hence the analysis of this paper was undertaken to document the derivation of pertinent equations, using conservation of mass and energy. Note that since the analysis is limited to determining radiator area requirements for specified mass flow rates and temperatures, but not radiator pressure drop, only conservation of mass and energy relationships were considered. Since the momentum equation was not required for the determination of radiator area, it is not included in the analysis. The results are in agreement with earlier work by the author (Juhasz 2005) which integrates radiator heat rejection with CBC performance and mass analysis.

Applicability of Analysis to CBC Configurations

The mathematical derivations for analyzing the space heat rejection process, including the determination of total radiator area and wall surface temperature profile are valid for various CBC configurations as suggested by figures 1 and 2. The relationship of the *direct heat rejection radiator* for a non-regenerated system with direct heating by means of a high temperature gas reactor is illustrated by the cycle schematic of figure 1. Cycle heat rejection occurs by the gaseous working fluid flowing over evaporator sections of heat pipes whose finned condenser sections radiate to space. In contrast *the indirect heat rejection* scheme shown in figure 2 comprises transfer of heat by means of a heat exchanger from the gaseous cycle working fluid to an arbitrary radiator coolant fluid which is a pumped liquid.

The heat transfer within the radiator is now from the liquid radiator coolant flowing over the heat pipe evaporators and the final heat transfer step from the finned heat pipe condensers by thermal radiation is analogous to the "direct heat rejection" case of figure 1.

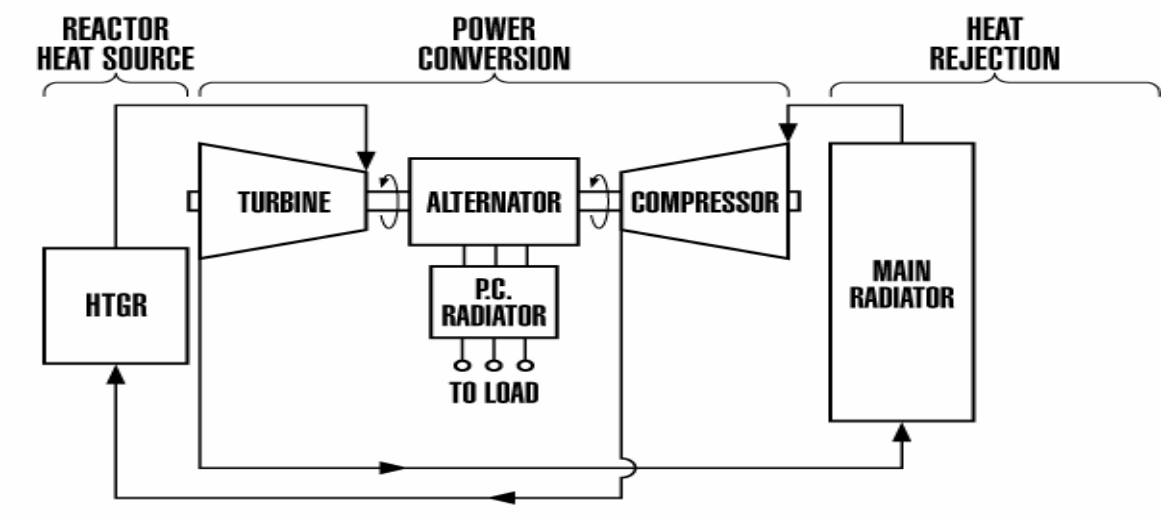

Figure 1.—Direct heat rejection radiator for non-regenerated closed Brayton cycle power system.

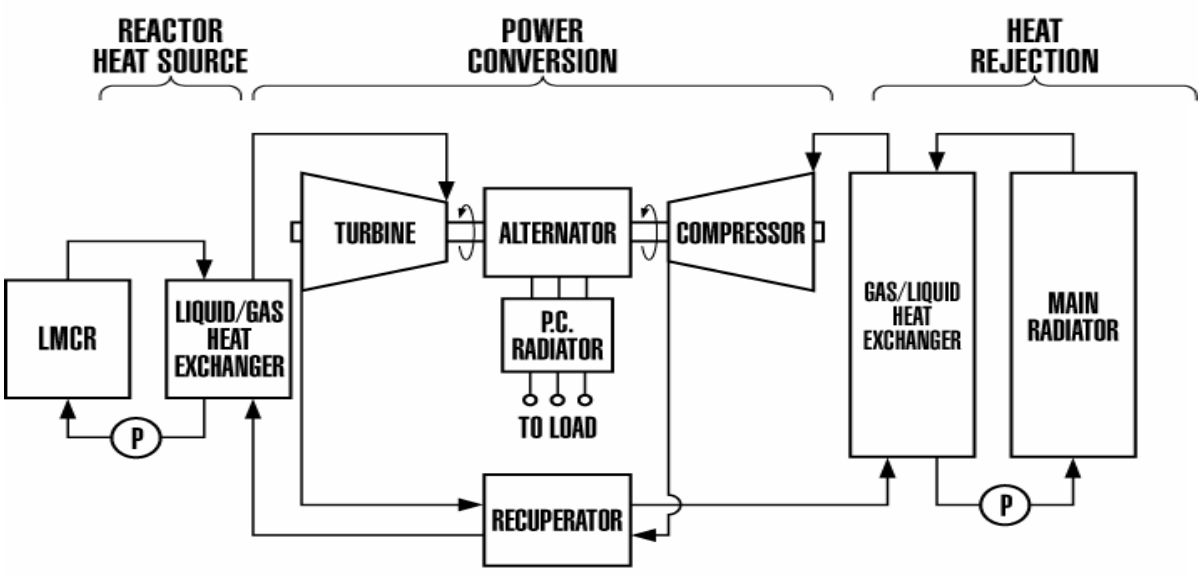

Figure 2.—In-direct heat rejection radiator for regenerated closed Brayton cycle power system.

Derivation of Radiator Energy Balance Equations

Fluid and Wall Temperatures

A one-dimensional model of a fluid being cooled while flowing in a closed duct whose outer surface rejects heat to the space environment by thermal radiation is suggested by figure 3, which is intended to show that a gas, or liquid, cooled by thermal radiation using heat pipes can be analyzed as simple one-dimensional diabatic flow in a constant area duct.

For an elemental radiator length the heat transferred from the fluid to the outer wall must equal the heat radiated from the outer wall to the space sink. Hence, we can write:

$$h_i (T - T_w) dA_i = \sigma \cdot \varepsilon \cdot F \cdot \left(T_w{}^4 - T_s{}^4 \right) \cdot dA_r \tag{1}$$

A fluid convective heat transfer coefficient related to the radiating area is defined as

$$h_r = h_i \cdot \frac{dA_i}{dA_r} \tag{2}$$

Using equation (2), equation (1) can be solved for the fluid temperature T, giving:

$$T = T_w + \frac{\sigma \cdot \varepsilon}{h_r} \cdot \left(T_w{}^4 - T_s{}^4 \right) \tag{3}$$

Implicit differentiation of (3) results in:

$$dT = \left(\frac{4 \cdot \sigma \cdot \varepsilon}{h_r} \cdot T_w{}^3 + 1 \right) \cdot dT_w \tag{4}$$

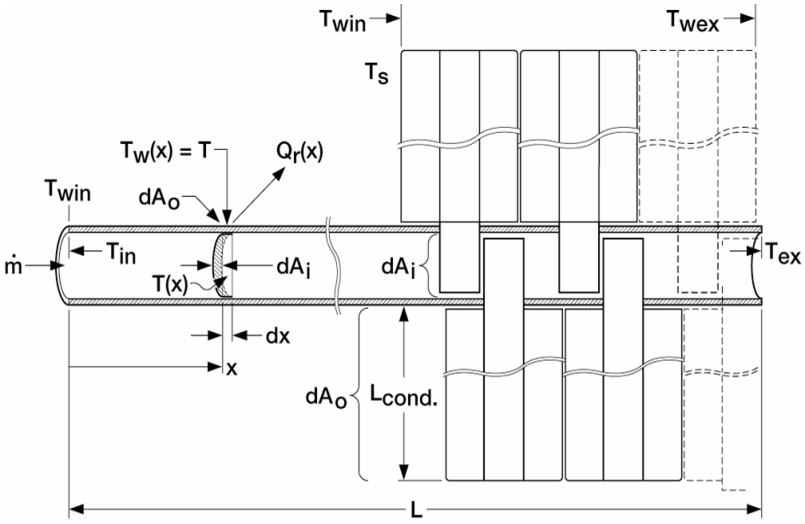

Figure 3.—Analogy of radiation cooled gas flow inside a 1–D duct to flow over heat pipe evaporators.

Note that with fluid temperature T known eqs. (3) and (4) are used to solve for T_W via a Newton-Raphson iteration.

A one-dimensional heat balance over an incremental section of the radiator, dA_r expresses the equivalence of a liquid or perfect gas enthalpy drop to the thermal radiation heat loss by the same incremental area, dA_r .

$$-\dot{m}\cdot C_p\cdot dT=\sigma\cdot\varepsilon\cdot\left(T_w{}^4-T_s{}^4\right)\cdot dA_r \tag{5}$$

Where $\dot{m}$ is the radiator fluid mass flow rate

C_p is the fluid specific heat; where $C_p=\dfrac{R\cdot\gamma}{\gamma-1}$ for a perfect gas

R is the Gas Constant $R=\dfrac{R_u}{Mol.Wt}$ and γ is the specific heat ratio $R_u=8314.34\dfrac{Joule}{kmol-K}$ is the Universal Gas Constant

Determination of Incremental and Total Radiator Area

Substituting equation (4) into equation (5) yields the following expression

$$-\dot{m}\cdot C_p\cdot\left(\frac{4\cdot\sigma\cdot\varepsilon\cdot T_w{}^3}{h_r}+1\right)\cdot dT_w=\sigma\cdot\varepsilon\cdot\left(T_w{}^4-T_s{}^4\right)\cdot dA_r \tag{6}$$

Solving equation (6) for dA_r results in

$$dA_r=-\dot{m}\cdot C_P\cdot\left[\frac{4\cdot T_w{}^3}{h_r\cdot\left(T_w{}^4-T_s{}^4\right)}+\frac{1}{\sigma\cdot\varepsilon\cdot\left(T_w{}^4-T_s{}^4\right)}\right]\cdot dT_w \tag{7}$$

The Integral of equation (7) over the entire radiator between the radiator outlet and inlet wall temperatures, T_{wex} and T_{win}, respectively, can be expressed as

$$\int_0^{A_r}1dA_r=-\dot{m}\cdot C_P\int_{T_{win}}^{T_{wex}}\left[\frac{4\cdot T_w{}^3}{h_r\cdot\left(T_w{}^4-T_s{}^4\right)}+\frac{1}{\sigma\cdot\varepsilon\cdot\left(T_w{}^4-T_s{}^4\right)}\right]dT_w \tag{8}$$

Although the first term in brackets of equation (8) can be readily integrated, one needs to resort to the method of partial fractions to integrate the second term. The integration steps are

$$A_r=\dot{m}\cdot C_p\cdot\left[\frac{(-1)}{h_r}\cdot\ln\left(T_w{}^4-T_s{}^4\right)\Big|_{T_{win}}^{T_{wex}}-\int_{T_{win}}^{T_{wex}}\frac{1}{\sigma\cdot\varepsilon\cdot\left(T_w{}^4-T_s{}^4\right)}dT_w\right] \tag{9}$$

which leads to the final expression for A_r as shown in equation (10), after substituting the indicated integration limits.

$$A_r = \dot{m}\cdot C_p \cdot \left[\frac{1}{h_r}\cdot \ln\left(\frac{{T_{win}}^4 - {T_s}^4}{{T_{wex}}^4 - {T_s}^4} \right) + \frac{1}{\left(4\cdot\sigma\cdot\varepsilon\cdot {T_s}^3\right)} \cdot \left[\ln \frac{(T_{win}-T_s)\cdot(T_{wex}+T_s)}{(T_{wex}-T_s)\cdot(T_{win}+T_s)} - 2\cdot\left(\tan^{-1}\cdot\frac{T_{win}}{T_s} - \tan^{-1}\cdot\frac{T_{wex}}{T_s} \right) \right] \right] \tag{10}$$

Radiator Area Fraction to Reach a Specified Wall Temperature

A powerful feature concerning equations (8), (9), and (10) needs to be mentioned. If one is interested in determining the fractional radiator area $A_r(x)$ to a region where the wall temperature reaches a specified value, $T_w(x)$ where $T_{wex} \le T_w(x) < T_{win}$ then the equation (9) can be integrated between upper and lower limits of $T_w(x)$ and Twin

$$\int_0^{A_r(x)} dA_r = -\dot{m}\cdot C_P \cdot \int_{T_{win}}^{T_w(x)} \left[\frac{4\cdot\sigma\cdot\varepsilon\cdot {T_w}^3}{h_r\cdot\left({T_w}^4 - {T_s}^4\right)} + \frac{1}{\sigma\cdot\varepsilon\cdot\left({T_w}^4 - {T_s}^4\right)} \right] dT_w \tag{11}$$

Evaluation of the integral shown in equation (11) will result in an expression for $A_{r(x)}$, which is similar to equation (10), but for the T_{wex} symbols being replaced by $T_w(x)$. To determine the fractional distance, *x*, along the radiator where the wall temperature reaches $T_w(x)$, one can take the ratio of areas to obtain:

$$x = \frac{\ln\left(\frac{{T_{win}}^4 - {T_s}^4}{{T_w(x)}^4 - {T_s}^4} \right) + \frac{1}{\left(4\cdot\sigma\cdot\varepsilon\cdot {T_s}^3\right)} \cdot \left[\ln\cdot \frac{\left(T_{win}-T_s\right)\cdot\left(T_w(x)+T_s\right)}{\left(T_w(x)-T_s\right)\cdot\left(T_{win}+T_s\right)} - 2\cdot\left(\tan^{-1}\cdot\frac{T_{win}}{T_s} - \tan^{-1}\cdot\frac{T_w(x)}{T_s} \right) \right]}{\ln\left(\frac{{T_{win}}^4 - {T_s}^4}{{T_{wex}}^4 - {T_s}^4} \right) + \frac{1}{\left(4\cdot\sigma\cdot\varepsilon\cdot {T_s}^3\right)} \cdot \left[\ln\cdot \frac{\left(T_{win}-T_s\right)\cdot\left(T_{wex}+T_s\right)}{\left(T_{wex}-T_s\right)\cdot\left(T_{win}+T_s\right)} - 2\cdot\left(\tan^{-1}\cdot\frac{T_{win}}{T_s} - \tan^{-1}\cdot\frac{T_{wex}}{T_s} \right) \right]} \tag{12}$$

Equation (12) can be used to compute the fraction of total radiator area bounded by specified wall temperatures, in order to determine the weight of multi-segment radiators built from different materials as dictated by wall temperature requirements.

A mean effective radiator wall temperature T_{weff} can be derived by substituting equation (10) into a heat balance for the entire radiator, namely:

$$\dot{m}\cdot C_p\cdot\left(T_{in} - T_{ex}\right) = \sigma\cdot\varepsilon\cdot A_r\cdot\left({T_{weff}}^4 - {T_s}^4\right) \tag{13}$$

where T_{in} and T_{ex} are the working fluid inlet and outlet temperatures, respectively. Solving equation (13) for T_{weff} one obtains:

$$T_{weff} = \left[\dot{m} \cdot C_P \cdot \frac{(T_{in} - T_{ex})}{(\sigma \cdot \varepsilon \cdot A_r)} + T_s{}^4 \right]^{0.25} \tag{14}$$

All values on the right hand side of equation (14) are known, except for the fluid temperatures T_{in} and T_{ex}. But these can be expressed in terms of the corresponding wall temperatures by using the relationships given in equation (3):

$$T_{in} = T_{win} + \frac{\sigma \cdot \varepsilon}{h_r} \cdot \left(T_{win}{}^4 - T_s{}^4 \right) \tag{15}$$

and

$$T_{ex} = T_{wex} + \frac{\sigma \cdot \varepsilon}{h_r} \cdot \left(T_{wex}{}^4 - T_s{}^4 \right) \tag{16}$$

Finally substituting equations (A15) and (16) into equation (14) the following expression is obtained for T_{weff}

$$T_{weff} = \left[T_s{}^4 + \frac{\dot{m} \cdot C_p}{\sigma \cdot \varepsilon \cdot A_r} \cdot \left[T_{win} - T_{wex} + \frac{\sigma \cdot \varepsilon}{h_r} \cdot (T_{win} - T_{wex}) \right] \right]^{0.25} \tag{17}$$

Equation (17) is the "mean effective"—or integrated wall temperature of a duct which is carrying a radiatively cooled liquid or gaseous working fluid with known heat transport properties.

Note that, although the above analysis has been performed with the assumption that the heat transfer coefficient, h_r, is constant throughout the duct, it is possible to include variable heat transfer conditions as discussed next.

The Case of Variable Heat Transfer Coefficients

For the case where the heat transfer coefficient is a function of temperature and duct position a finite difference computational approach was used. The duct was subdivided into n sections with running index j ranging from $j = 1$ to n, with each of these sections having a specified heat transfer coefficient, $h_r(j)$ controlling the internal heat transfer process over section j. Equation (11) can then be rewritten as

$$\int_{A_r(j)}^{A_r(j+1)} dA_r = -\dot{m} C_p \int_{T_w(j)}^{T_w(j+1)} \left[\frac{4 \cdot \sigma \cdot \varepsilon \cdot T_w^3}{h_r(j) \cdot (T_w^4 - T_s^4)} + \frac{1}{\sigma \cdot \varepsilon \cdot (T_w^4 - T_s^4)} \right] dT_w \text{ -} \tag{18}$$

The total required heat transfer area may then be found by summing the elemental areas in accordance with equation (18) from element j to element n, as shown below.

$$A_{tot} = \sum_{j=1}^{n} \int_{A_r(j)}^{A_r(j+1)} dA_r \tag{19}$$

Equations (18) and (19) were programmed in the radiator subroutine and validated by subdividing the radiator into 25 sub-sections each having identical heat transfer coefficients, $h_r(j)$. Performing the summation indicated by equation (19) the same total area was obtained as for the integral (non-sectioned) radiator having the same internal heat transfer coefficient.

When substituting monotonically increasing heat transfer coefficients in the sectioned radiator configuration, the result was a reasonable reduction in total area of ~3 percent.

Temperature Profile Example

An illustration of a wall temperature profile resulting from a given radiator fluid temperature distribution and with a gradually increasing *h* as the flow proceeds from the radiator duct inlet to exit will be more meaningful if comparative wall temperature profiles with constant *h* are also shown on the same plot as illustrated in figure 4, which shows four "Mathcad" generated curves. The radiator conditions are typical for a hypothetical high turbine inlet temperature of 2000 K, with a cycle temperature ratio of 3.5 and a pressure ratio of 2.0 for a regenerated cycle.

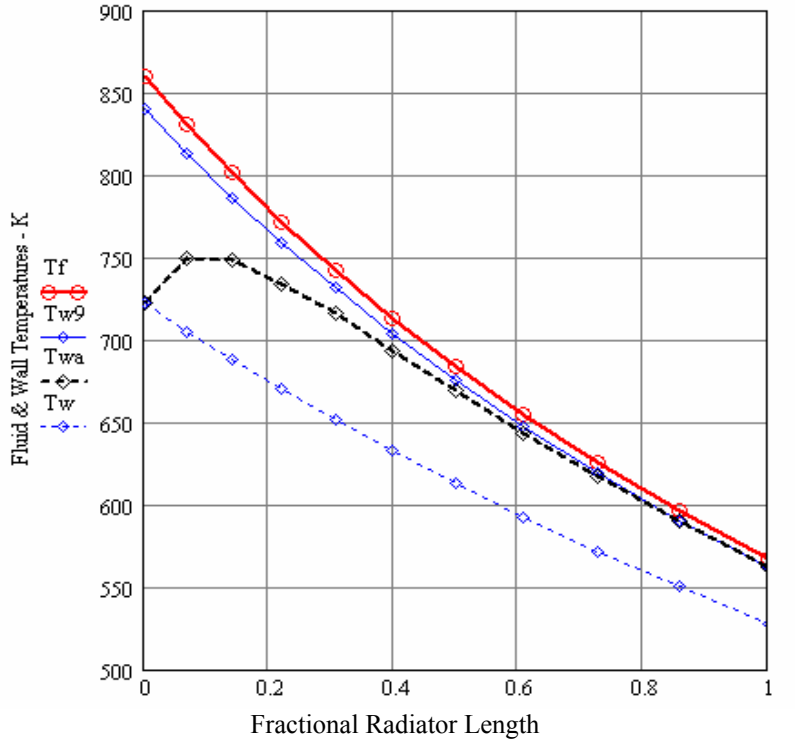

Figure 4.—Fluid and wall temperature profiles for various internal heat transfer coefficients.

The top curve with the circle symbols, marked Tf, represents a given He gas temperature profile with a duct inlet temperature of ~860 K and an exit temperature of 567 K. The second curve from the top, T_w9, with the diamond symbols shows a corresponding wall temperature profile obtained with a very high constant heat transfer coefficient, $h = 1300\ W/m^2 - K$. In contrast, the bottom dashed curve (also with diamond symbols, but marked T_w) represents a wall temperature profile for an assumed value of $h = 100\ W/m^2 - K$. The third, heavy dashed curve from the top, Twa, depicts the wall temperature profile resulting from flow conditions in which the value of *h* increases monotonically from 100 to $1300\ W/m^2 - K$. Note that the wall temperature values for this curve agree with the duct entrance value for the low and the duct exit value for the high heat transfer case. It is also of interest to note that the variable

heat transfer wall temperature profile approaches the wall temperature profile of the high heat transfer case asymptotically at the duct exit. This fact provides an important validation check on the correctness of the computational procedure inherent in the author's radiator sub-program.

A typical example of the influence of variable heat transfer coefficients on the conceptual design of a trapezoidal heat pipe radiator for a CBC energy conversion system with a fission reactor heat source is discussed in the next section.

Application of Analysis to Conceptual Design of a Spacecraft Radiator

In the derivation of the radiator heat balance equations a fundamental assumption was that the radiator fluid convective heat transfer coefficient can be related to the radiating area by equation (2), namely

$$h_r = h_i \cdot \frac{dA_i}{dA_r} \tag{20}$$

Concerning the ratio of differential areas, dA_i / dA_r, it is evident from figure 3 that this ratio is identical to the ratio of heat pipe evaporator area inside the duct, which is exposed to the working fluid, to the finned condenser area external to the duct, which is exposed to the vacuum of space.

As an illustrative example figure 5 shows the trapezoidal radiator panels proposed for the SP–100 conical radiator configuration. Assume that the radiator cooling fluid enters the central duct at the lower right of the trapezoidal panel. Furthermore, a constant evaporator length of ~0.2 meters (i.e., for 100 kWe BC power system) throughout the duct and a gradually decreasing finned HP condenser length from 0.6 m at the duct entrance to 0.2 m at the exit are assumed. Thus the incremental area ratio is obviously increasing from 0.333 to 1.0. This means that for constant h_i the value of h_r will increase by a factor of three, even if the duct cross sectional flow area is constant. Of course the opposite trend is obtained for radiator working fluid entering the central duct at the short end of the trapezoid panel. In this case, for a constant value of h_i, the value of h_r will decrease by a factor of three. The preferred flow direction for minimizing radiator area will be discussed in the next paragraphs using the theoretical relationships developed above.

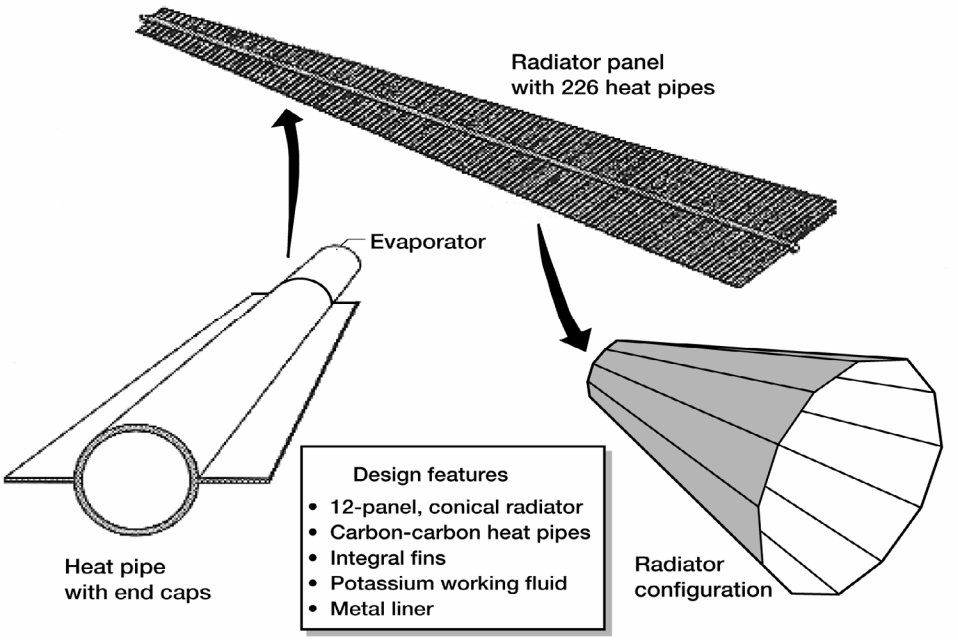

Figure 5.—SP–100 trapezoidal radiator panel and conical radiator assembly.

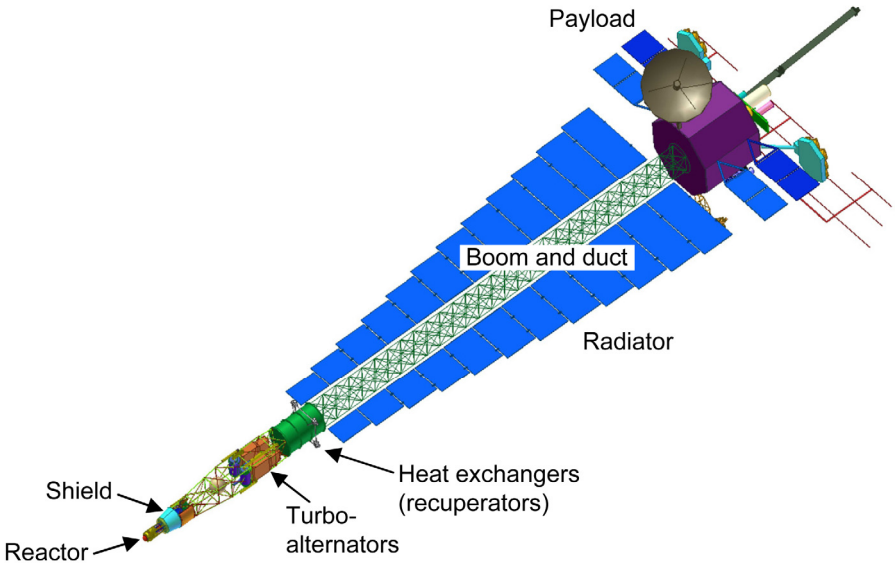

Figure 6.—Nuclear-CBC powered spacecraft with trapezoidal HP radiator.

Of course, for nuclear space power systems the trapezoidal radiator panel shape is dictated by the requirement that the radiator fits inside the "shadow" of a radiation shield which is placed between the reactor and the spacecraft major components, in order to reduce radiation dose levels (i.e., Neutron and gamma) on the power system, radiator, and the payload. Such a conceptual nuclear power system comprising a fission reactor with a neutron-gamma "shadow shield," and a CBC power system with a flat panel trapezoidal radiator is shown in figure 6. This figure a conceptual diagram of a 100 kWe class space nuclear power system using regenerated CBC conversion technology with the main sub-systems are also identified. Note the large trapezoidal area devoted to the radiator which is in the shadow of a conical shield of 15° half angle.

In this system the best upstream point for fluid entry is hypothesized to be at the end where the finned heat pipe condenser section is longest, since the heat transfer coefficient, h_r, would be lowest where the radiator fluid temperature is highest. As the radiator fluid proceeds downstream toward the compressor inlet, the fluid temperature decreases, but h_r is rising, since the ratio dA_i/dA_r in equation (2) is increasing. After the gas has been cooled to compressor inlet temperature at the radiator duct exit, it is piped near isothermally in the same direction for re-injection into the compressor.

To verify the above hypothesis, the derived relationships (especially eq. (18)) were programmed into a numerical code which was then used to perform radiator area calculations for the fluid temperature profile shown in figure 4, and a total heat load of 199 kW_t. The computational results for three heat transfer coefficient input cases are summarized in table I.

TABLE I.—RADIATOR PANEL AREA COMPARISONS FOR 3 DIFFERENT INTERNAL HEAT TRANSFER CASES[a]

Case number	Heat transfer coeff, h_r, W/m^2-K	Specific radiator panel area, m^2/kWe	Radiator area change, percent	Remarks
1	200 – Constant	0.24453	0.	Rectangular Radiator panel
2	600 to 200 decreasing	0.22384	–8.46	Trapezoidal panel Entry @ short end
3	200 to 600 increasing	0.22099	–9.63	Trapezoidal panel Entry @ long end

[a]Total heat rejected = 199 kWt; Duct Inlet Temp. = 859.3 K; Duct Exit Temp. = 570 K; Space Sink Temp. = 200 K
Radiator duct divided into 21 segments in flow direction.

The following conclusions can be drawn from the three cases shown in this table for the conditions indicated by the asterisk:

(1) For the case of a constant heat transfer coefficient of 200 W/m^2-K the specific radiator panel area was computed at 0.2445 m^2/kWe. This value was used as a reference for comparison with cases 2 and 3.

(2) Case 2 represents a trapezoidal radiator panel with flow entering the radiator duct on the short side, as was done for the SP–100 panels. The heat transfer coefficient, h_r, was varied from 0.6 to 0.2 kW/m^2–K linearly in 21 steps with the direction of the radiator working fluid which in this case was identical with the helium gas turbine working fluid. The required panel area is seen to decrease by 8.46 percent.

(3) Case 3 represents a trapezoidal radiator panel with flow entering the radiator duct on the long side, as is recommended by this author, since this would cause h_r to increase from 0.2 to 0.6 kW/m^2–K. As a result the radiator area reduction would further improve from 8.46 to 9.63 percent, as shown. Although the improvement over case 2 is only a modest ~1.2 percent, the actual area savings would be significant for high power systems requiring several thousand square meters of radiator area.

The results shown in table I show that, as hypothesized, it would be of some advantage to send the flow along the central boom to the wide end of the trapezoid, where the finned heat pipe condensers are longest and the radiator fluid temperature is highest, and have it enter the duct at this point so that thermal energy transfer can occur with gas flowing over the heat pipe evaporators in a direction towards the turbo-alternator.

Conclusions

A detailed derivation of the mathematical relationships governing heat rejection from a CBC space power system was completed. The analysis is valid for both systems having a separate liquid pumped heat rejection loop connected to the CBC by means of a gas-to-liquid heat exchanger, or direct heat rejection by the cycle working fluid flowing over evaporator sections of heat pipes which protrude into a closed heat transport duct. The analysis also showed that designing the radiator duct in a manner that will allow the effective heat transfer coefficient to increase in the direction of the flow will result in a modest decrease in radiator area requirements.

Although the analysis was motivated by the heat rejection process of CBC power systems, it can be extended to computing surface area and weight of any gas-or liquid cooled space radiator as long as required input conditions are known.

Nomenclature

A_i	inner surface area; A_o outer surface area
$A_{r(j)}$	incremental radiator area at section j
dA_i	elemental inner wall surface, or heat pipe evaporator area
dA_r	dA_O, is the elemental radiating outer wall surface, or heat pipe condenser area
C_p	fluid specific heat; where $C_p = \frac{R \cdot \gamma}{\gamma - 1}$ for a perfect gas
F	is the view factor to the space environment (F = 1 for this analysis)
h	heat transfer coefficient
h_i	internal heat transfer coefficient

h_r	heat transfer coefficient normalized to external or radiating area
$\dot{m}$	radiator fluid mass flow rate
R	Gas constant $\left(R = \frac{R_u}{Mol.Wt} \right)$; R_u = Universal Gas Constant = 8314.34 Joule/(kmol–K)
T_{wex}	wall temperature at duct outlet
T_{win}	wall temperature at duct inlet
$T = T(x)$	is the fluid bulk temperature at axial location x
$T_S = T_{space}$	is the equilibrium space sink temperature
$T_w = T_w(x)$	$T_{w(j)}$ wall temperature at arbitrary location x, or *j*
T_{weff}	effective radiator wall temperature
x	fractional distance along radiator flow path
γ	specific heat ratio of radiator heat transport fluid
σ	the Stefan-Boltzmann constant = 5.668×10^{-8} watts/m^{2}K^4
ε	the emissivity of the radiating surface

References

Juhasz, Albert J., "An Analysis and Procedure for Determining Space Environmental Sink Temperatures with Selected Computational Results," NASA/TM—2001-210063, Jan. 2001.

Juhasz, A.J., "Analysis and Numerical Optimization of Gas Turbine Space Power Systems with Nuclear Fission Reactor Heat Sources," Doctoral Dissertation, Cleveland State University, May 25th, 2005.

Juhasz, A.J. and Sawicki, J.T., "Lunar Surface Power Systems with Fission Reactor Heat Sources," NASA/TM—2005-214003, Nov. 2005.

Juhasz, A.J., "Multi-Megawatt Gas Turbine Power Systems for Lunar Colonies," NASA/TM—2006-214658, Dec. 2006

Klann, John L., "Steady State Analysis of a Brayton Space Power System," NASA TN D–5673, Feb. 1970

Truscello, V.C. and Rutger, "The SP–100 Power System" in Proceedings of the Ninth Symposium on Space Nuclear Power Systems, Albuquerque, NM, Jan. 1992

REPORT DOCUMENTATION PAGE	Form Approved OMB No. 0704-0188

1. REPORT DATE *(DD-MM-YYYY)*	2. REPORT TYPE	3. DATES COVERED *(From - To)*
01-08-2007	Technical Memorandum	

4. TITLE AND SUBTITLE
Heat Transfer Analysis of a Closed Brayton Cycle Space Radiator

5a. CONTRACT NUMBER

5b. GRANT NUMBER

5c. PROGRAM ELEMENT NUMBER

6. AUTHOR(S)
Juhasz, Albert, J.

5d. PROJECT NUMBER

5e. TASK NUMBER

5f. WORK UNIT NUMBER
WBS 463169.01.03

7. PERFORMING ORGANIZATION NAME(S) AND ADDRESS(ES)
National Aeronautics and Space Administration
John H. Glenn Research Center at Lewis Field
Cleveland, Ohio 44135-3191

8. PERFORMING ORGANIZATION REPORT NUMBER
E-16193

9. SPONSORING/MONITORING AGENCY NAME(S) AND ADDRESS(ES)
National Aeronautics and Space Administration
Washington, DC 20546-0001

10. SPONSORING/MONITORS ACRONYM(S)
NASA

11. SPONSORING/MONITORING REPORT NUMBER
NASA/TM-2007-215003

12. DISTRIBUTION/AVAILABILITY STATEMENT
Unclassified-Unlimited
Subject Categories: 20, 64, and 93
Available electronically at http://gltrs.grc.nasa.gov
This publication is available from the NASA Center for AeroSpace Information, 301-621-0390

13. SUPPLEMENTARY NOTES

14. ABSTRACT
This paper presents a mathematical analysis of the heat transfer processes taking place in a radiator for a closed cycle gas turbine (CCGT), also referred to as a Closed Brayton Cycle (CBC) space power system. The resulting equations and relationships have been incorporated into a radiator sub-routine of a numerical triple objective CCGT optimization program to determine operating conditions yielding maximum cycle efficiency, minimum radiator area and minimum overall systems mass. Study results should be of interest to numerical modeling of closed cycle Brayton space power systems and to the design of fluid cooled radiators in general.

15. SUBJECT TERMS
Space radiator; Brayton space power systems; Space heat rejection; Computational techniques

16. SECURITY CLASSIFICATION OF:			17. LIMITATION OF ABSTRACT	18. NUMBER OF PAGES	19a. NAME OF RESPONSIBLE PERSON
a. REPORT	b. ABSTRACT	c. THIS PAGE			STI Help Desk (email:help@sti.nasa.gov)
U	U	U	UU	17	19b. TELEPHONE NUMBER *(include area code)* 301-621-0390